International Journal of Nanomedicine

Dovepress

open access to scientific and medical research

Open Access Full Text Article

ORIGINAL RESEARCH

Oral Delivery of Pterostilbene by L-Arginine-Mediated "Nano-Bomb" Carrier for the Treatment of Ulcerative Colitis

Wei Wei[1–3], Yujie Zhang[1,2], Runqing Li[4], Yameng Cao[1,2], Xiangji Yan[1,2], Yana Ma[1,2], Yuanyuan Zhang[1,2], Mei Yang[1,2], Mingzhen Zhang[1,2]

[1]School of Basic Medical Sciences, Xi'an Key Laboratory of Immune Related Diseases, Xi'an Jiaotong University, Xi'an, Shaanxi, People's Republic of China; [2]Key Laboratory of Environment and Genes Related to Diseases, Ministry of Education, Xi'an Jiaotong University, Xi'an, Shaanxi, People's Republic of China; [3]Xi'an No.1 Hospital, Shaanxi Institute of Ophthalmology, Shaanxi Key Laboratory of Ophthalmology, Clinical Research Center for Ophthalmology Diseases of Shaanxi Province, First Affiliated Hospital of Northwestern University, Xi'an, Shaanxi, People's Republic of China; [4]Department of Radiology, The First Affiliated Hospital of Xi'an Jiaotong University, Xi'an, Shaanxi, People's Republic of China

Correspondence: Mei Yang; Mingzhen Zhang, Email yangmeimei528@stu.xjtu.edu.cn; mzhang21@xjtu.edu.cn

Background: Ulcerative colitis (UC) is a chronic inflammatory bowel disease (IBD) of unknown aetiology affecting the colon and rectum. Pterostilbene (PS) has been reported as an effective antioxidant and anti-inflammatory agent in preclinical IBD models. However, the therapeutic outcomes of PS are limited by potential side effects associated with the systemic exposure and the modest bioavailability afforded by its oral administration. These issues can be improved with the use of intelligent responsive nanoparticles with the ability of lysosome escape, given their high drug delivery capacity and reducing the side effects.

Materials and Methods: Herein, the hyaluronic acid (HA)-modified L-arginine CO_2 nanoparticles (HA-L-Arg-CO_2@NPs) loaded with PS (HA-PS@NPs) are constructed. Under lysosomal pH conditions, HA-PS@NPs liberate CO_2 and generate a pH-activated nano-bomb effect to augment the cytosolic delivery of PS.

Results: HA-L-Arg-CO_2@NPs show great biocompatibility and the excellent ability to target the colon. Using lipopolysaccharide-induced inflammation in vitro, the prominent anti-inflammatory effect of HA-L-Arg-CO_2@NPs and HA-PS@NPs is observed. Further, orally administered HA-L-Arg-CO_2@NPs and HA-PS@NPs via the colon-targeted chitosan/alginate (CA) hydrogel downregulate pro-inflammatory cytokines and reduce intestinal permeability, yielding significant outcomes in alleviating the symptoms of UC.

Conclusion: This pH-activated "nano-bomb" carrier with therapeutic effect can be exploited as efficient oral drug carriers for UC treatment.

Keywords: ulcerative colitis, pterostilbene, nano-bomb effect, L-arginine, oral administration

Introduction

Ulcerative colitis (UC), a subcategory of inflammatory bowel disease (IBD), is a chronic idiopathic intestinal inflammatory disease with unknown etiology. The continuous diffuse inflammation and damage in the colon is a distinguishing feature of UC.[1,2] There is evidence that UC is mainly characterized by the imbalance of T helper (Th)17 and regulatory T (Treg) cells dominated T lymphocyte response, and mucosa cytokine (TNF-α, IL-6, IL-1β) responses resulted in diffuse atrophic changes in crypts and the mucosal layer. The goal of clinical treatment is first to induce remission and then maintain a corticosteroid-free remission.[3–5] Commonly used drugs in clinical, including 5-aminosalicylic acid, corticosteroids, immunosuppressive drugs, and biological agents, are mainly limited to the relief of long-term symptoms and side effects due to insufficient targeting ability, which seriously reduces the quality of life of patients.[6–8] Therefore, there is a great need for targeted delivery systems, which can localize the drugs in the inflamed colon with minimum systemic distribution and side effects.

Received: 8 November 2021
Accepted: 25 January 2022
Published: 9 February 2022

Nowadays, nanoparticles have been increasingly used as drug carriers and diagnostic or therapeutic agents in medicine.[9–11] However, the typically uptake of the nanoparticles-based delivery systems into cells is via endocytosis into endo/lysosomes and then subsequently trafficked into acidic lysosomal compartments, while the environment of lysosome results in significant degradation of the therapeutic cargo.[12] This significantly reduces the efficiency of drug delivery. The pH-responsive nano-bomb delivery system could mitigate the degradation of enzymes in lysosomes and significantly improve the efficiency of drugs to cytoplasm. However, the synthesis of agents with nano-bomb effect as previously reported, such as chitosan-guanidine,[13,14] metal−phenolic networks,[15] or cell-penetrating peptides (CPPs),[16] is complex and highly costly, and it has no therapeutic effect on inflammation. Therefore, novel, simple, economical, and mass-produce nano-bomb systems need to be designed.

L-arginine (L-Arg) is a semi-essential amino acid, and most importantly, it contains natural guanidine groups, which are the natural requisite with bomb effect. Guanidine group adsorbs CO_2 in neutral pH conditions and release CO_2 in lysosome acidic pH conditions, so that the emitted CO_2 can break lysosomes into leakage payloads. Furthermore, there is evidence that L-Arg metabolism plays an important regulatory role and could be used as adjunctive therapy in colitis.[17–21] Pterostilbene (3,5-dimethoxy-4'-hydroxystilbene) (PS), a dimethyl ester analog of resveratrol, has anti-inflammatory and antioxidative effects as well as alters cell proliferation.[22] Multiple evidence showed that PS significantly attenuated visible damage and histological injury in ulcerative colitis (UC) animals via inhibition of NF-κB and activation of PPAR-γ.[23]

In this work, we aimed to construct an HA-modified L-Arg-based pH-activated nano-bomb system loaded with PS (HA-PS@NPs) for the treatment of UC. Firstly, we synthesized hyaluronic acid (HA) modified "nano-bomb effect" NPs (HA-L-Arg-CO_2@NPs) loaded with Pterostilbene (PS) (HA-PS@NPs). For surviving in the harsh gastrointestinal environment and targeting to colon, HA-PS@NPs were loaded in chitosan/alginate (CA) hydrogel for site-specific oral delivery to the inflamed colon via CD44-involved endocytosis (Figure 1). The chitosan/alginate (CA) hydrogel is based on the association of two polysaccharides, alginate and chitosan, which is usually employed as a carrier for colon-specific drug delivery. Alginate and chitosan form gels that chelate with a calcium or sulfate solution, respectively.[24–27] And the chitosan also has therapeutic effects on inflammatory cells in the colon.[28] L-Arginine-CO_2 (L-Arg-CO_2) loaded in NPs was supposed to release CO_2 under lysosomal pH to produce the "nano-bomb effect", which triggered L-Arg and PS lysosomal escape. The released L-Arg and PS alleviated colonic inflammation by downregulating the expression of pro-inflammatory cytokines and the production of ROS. These results will have great potential to provide a new drug carrier for UC therapy.

Methods

Synthesizing of the NPs with "Nano-Bomb" Effect

NPs were synthesized using a double-emulsion technique with the slight modification described in our previous work.[29–31] PLGA (36 mg) and PLGA-PEG-Mal (4 mg) with the ratio of 9:1, DPPC (10 mg), and Pterostilbene (5 mg) were dissolved in 2 mL of dichloromethane (DCM) (organic phase). To capture CO_2, L-Arginine-CO_2 (L-Arg-CO_2) was made by bubbling the aqueous L-Arginine solution for 1 h with CO_2. L-Arginine or L-Arg-CO_2 (30 mg/mL) were dissolved in 400 μL of DI water (aqueous phase). The organic phase and aqueous phase solutions were then transferred into a centrifuge tube (50 mL) for ultrasonic emulsification with a Branson 550 sonicator under the condition of 20% power for 1 min. Then, 4 mL of PVA solution (2.5%) was added into the emulsion and was further emulsified for 2 min over an ice bath. After rotary evaporation to remove DCM, the emulsion was further stirred at room temperature for 3 h. Finally, NPs were recovered by centrifugation (15,000 rpm, 15 min, at 4°C) and washed with DI water for three times.

To prepare hyaluronic acid (HA) modified NPs, the synthesized NPs and sulfhydryl modified hyaluronic acid were mixed and stirred overnight at room temperature and then lyophilized to obtain hyaluronic acid NPs (HA NPs). DiL, DiR or DiO loaded HA NPs were handled in the same procedures.

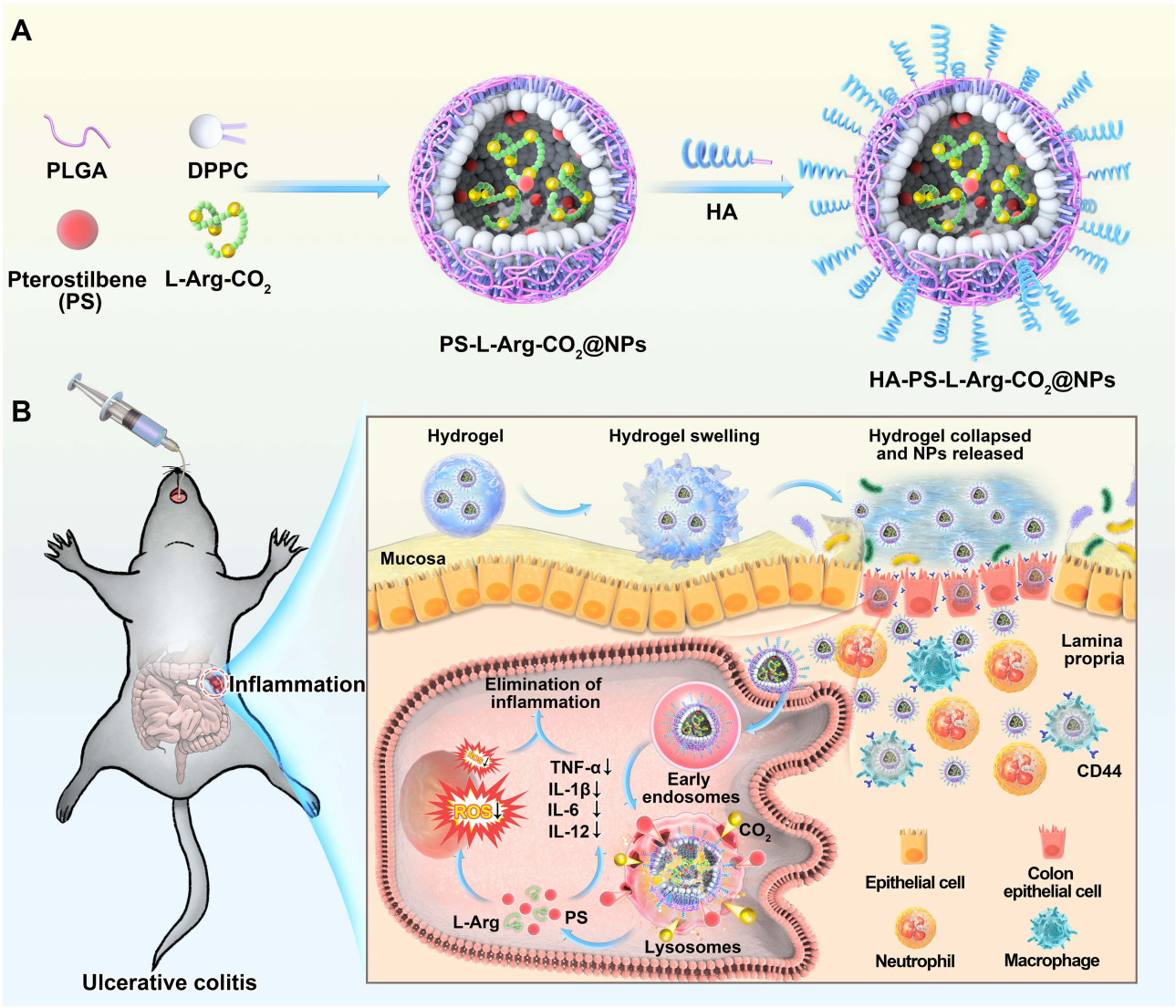

Figure 1 Schematic illustration of orally targeted delivery of L-Arginine based pH-activated "nano-bomb" carrier in hydrogel for site-specific treatment of ulcerative colitis. (**A**) PS-L-Arg-CO_2@NPs (NPs) with pH-activated "nano-bomb effect" were fabricated by double-emulsion technique. Then, the nanoparticles were linked with hyaluronic acid (HA) to endow their active targeting ability (HA-PS-L-Arg-CO_2@NPs, HA-PS@NPs). (**B**) HA-PS@NPs were loaded in chitosan/alginate hydrogel for site-specific treatment of ulcerative colitis by regulating gene silencing and the level of reactive oxygen species (ROS) via oral administration.

Preparation of Chitosan/Alginate (CA) Hydrogel

CA hydrogel was prepared according to the previous method.[24–27] Briefly, chitosan powder was dissolved in acetic acid and neutralized by adding 0.1 mol/L NaOH to form a solution with a final concentration of 0.6% (wt/vol). Sodium alginate was dissolved in 0.15 mol/L NaCl to create a solution with a final concentration of 1.4% (wt/vol). Finally, chitosan solution and sodium alginate solution were mixed in a ratio of 1:1, and the NPs above were added. 30 mM Na_2SO_4 and 70 mM $CaCl_2$ were prepared into a chelating solution with a volume of 2:1. The prepared chelating solution and hydrogel were incubated in a 37°C water bath, and then the chelating solution and polymer suspension were collected, respectively.

Animals

C57/BL6 female mice (8 weeks old) were provided by the Medical Experimental Animal Center of Xi'an Jiaotong University, Shaanxi Province, China. All experimental protocols involving animals were performed in accordance with

the Guidelines for Care and Use of Laboratory Animals of Xi'an Jiaotong University and approved by the Animal Ethics Committee of Xi'an Jiaotong University.

In vivo Intestinal Permeability Assay

FTIC-labeled dextran was used to evaluate mouse in vivo intestinal permeability.[32] Food and water were withdrawn for 4 hours, and then the mice were orally administered with FITC-labeled dextran (40 mg/100g body weight, Sigma). After 5 hours, the serum was collected, and fluorescence intensity in the serum was measured by a fluorescence spectrometer (excitation, 492nm; emission, 525nm; HITACHI, F-4700, Japan). FITC-dextran concentrations were determined using a standard curve generated by serial dilution of FITC-dextran.

Statistical Analyses

GraphPad Prism 7 was used to statistically analyze the data in this article. One-way and two-way analyses of variance (ANOVA) and t-tests were used to determine the statistical significance (*p<0.05, **p<0.01, ***p<0.001), p-values less than 0.05 were considered statistically significant.

Results

Preparation and Characterization of HA-PS@NPs

We designed a pH-activated nano-bomb drug delivery system by using a double emulsion solvent evaporation method based on the PLGA and L-Arg-CO_2 (Supplementary Methods). PLGA and DPPC formed the shell of the nanocarrier, and the core included PS and L-Arg-CO_2 (Figure 1). To verify the nano-bomb effect of the NPs, different methods were used to characterize their morphology (Supplementary Methods). Representative transmission electron microscope (TEM) images of L-Arg-CO_2@NPs showed that they had stable spherical core-shell structures at neutral pH (Figure 2A). In contrast, a few pores were present on the surface of some L-Arg-CO_2@NPs at pH 6.0, and more holes appeared almost on all NPs when the pH decreased to 5.0 (Figure 2A). The dynamic light scattering (DLS) method was used to measure the size and zeta potential of NPs at different conditions. L-Arg-CO_2@NPs had a diameter of 267.2 ± 1.38 nm, and there was no significant difference under different pH conditions (Figure 2B). The zeta potential of L-Arg-CO_2@NPs was −17.4±6.82 mV at pH 7.4 (Figure 2C). To further verify that the nano-bomb effect of NPs was caused by the CO_2 released from L-Arg-CO_2 under acidic pH conditions, we synthesized the L-Arg@NPs, which replaced L-Arg-CO_2 with L-Arg. Unlike L-Arg-CO_2@NPs, L-Arg@NPs maintained intact spherical core-shell structures under three different pH conditions (Figure S1a). The size and zeta potential of L-Arg@NPs were 279.9 ± 0.934 nm under different pH conditions and −21.5±5.83 mV (Figure S1b and c), respectively. The encapsulation efficiency and loading rate of PS measured by UV spectrophotometer were 79±4.58% and 11.67±1.42%, respectively. These results indicated that acidic pH-activated "nano-bomb" was successfully synthesized, in which CO_2 released from L-Arg-CO_2 encapsulated in the NPs could expand and/or break open the NPs to achieve the "nano-bomb" effect, and this bomb effects did not affect the encapsulation efficiency and loading rate of PS.

To enrich more NPs in the colon, we modified the surface of the NPs with hyaluronic acid (HA) through Michael addition reaction to target the CD44 receptor that was highly expressed in the inflammation site of the colon. After modification with HA, the spherical shell-core structure of the NPs was not affected (Figure 2D). The size and zeta potential of HA-L-Arg-CO_2@NPs (HA NPs) were changed from 279.9 ± 0.934 nm to 296 ± 0.24 nm and from −21.5 ±5.83 mV to −23.5±6.79 mV, respectively (Figure 2E and F). Owing to the low number of maleimide and sulfhydryl groups participating in the reaction, the results of FT-IR spectra showed that weak C-H near 1420 $cm^{-1}$and C-S stretching vibration of 1300 cm^{-1}accessories (Figure 2G). Combined with these results, we confirmed that HA was successfully conjugated to the surface of NPs.

HA-L-Arg-CO_2@NPs (HA NPs) Uptake and Intracellular Trafficking

To test whether cells ingested HA NPs in vitro, the 1,1'-dioctadecyl-3,3,3',3'-tetramethyl indocarbocyanine perchlorate (DiL)-labeled HA NPs were incubated with Colon-26 epithelial-like cells and activated Raw 264.7 cells (Supplementary

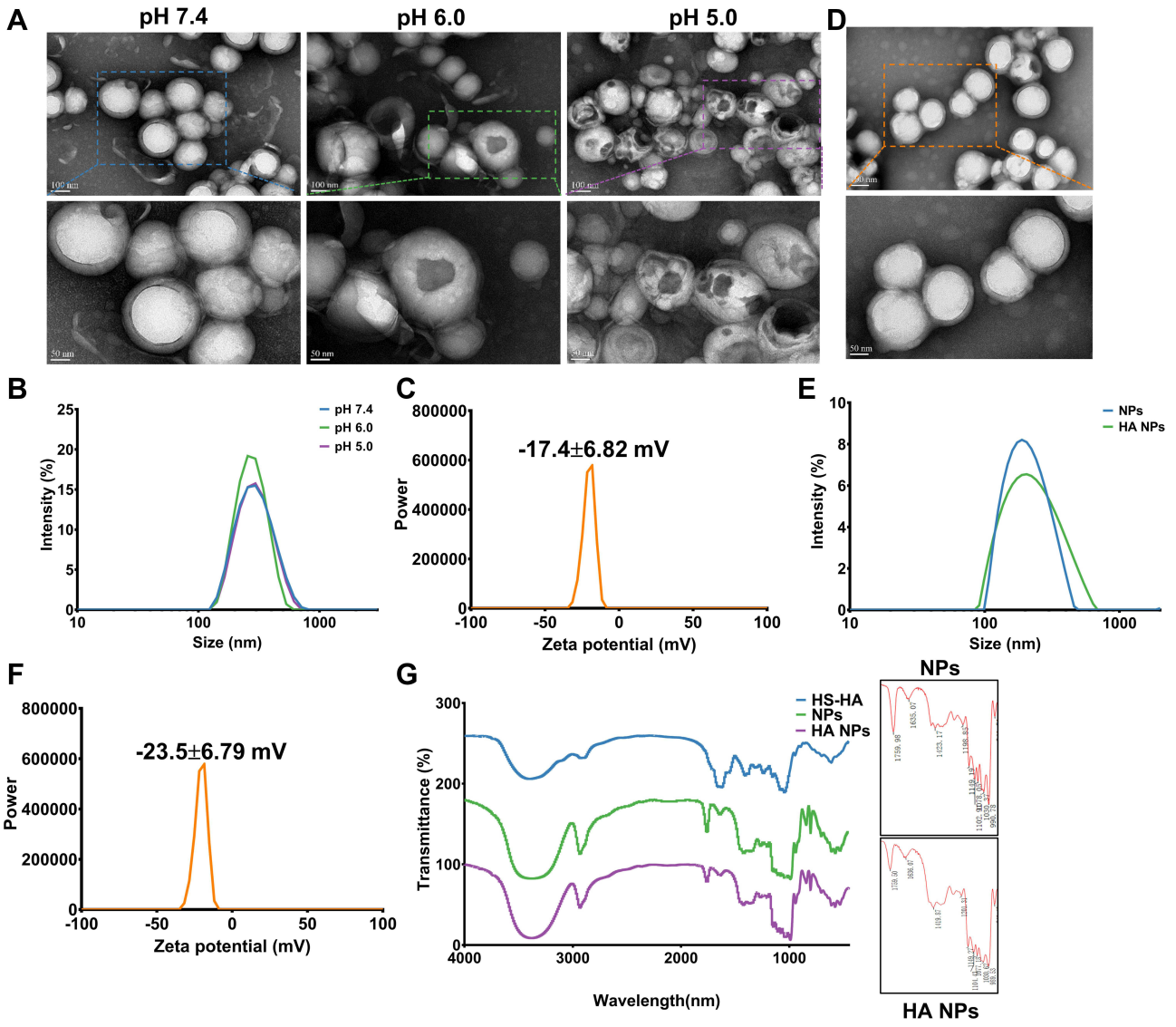

Figure 2 Synthesis and characterization of "nano-bomb effect" nanoparticles and hyaluronic acid (HA) modified with nanoparticles. (**A**) TEM images of the nanoparticles under different pH conditions for 3 h at 37°C (n=5). The nanoparticles maintain a spherical morphology and core-shell structure at pH 7.4, and were broken open under lower pH (pH 6.0 and pH 5.0), indicated the pH-activated behavior. (**B**) Size distribution of nanoparticles at different pH conditions were measured by dynamic light scattering (DLS) (n=5). (**C**) The zeta potential of nanoparticles was −17.4±6.82 mV, which was measured by dynamic light scattering (DLS) (n=5). (**D**) TEM images of L-Arg-CO_2@NPs modified with HA. (**E** and **F**) Size distribution and zeta potential of L-Arg-CO_2@NPs (NPs) and HA-L-Arg-CO_2@NPs (HA NPs) were determined by dynamic light scattering (DLS). (**G**) FT-IR spectra of HA-L-Arg-CO_2@NPs (HA NPs) showing the changes of infrared spectra of the Michael addition reaction between maleimide and sulfhydryl.

Abbreviation: FT-IR, Fourier transform infrared spectroscopy.

Methods). Confocal images showed that, compared with the control group, strong DiL signals on the cytoplasm or cell membrane surface of Colon-26 and Raw 264.7 cells in the HA NPs/DiL groups (Figure 3A and B). Furthermore, flow cytometry was used to test the efficiency of HA NPs uptake by Colon-26 and Raw 264.7 cells. Compared to the control, the flow cytometry results showed that Colon-26 and Raw 264.7 cells ingested almost all HA NPs/DiL (Figure 3C and D). These results illustrated that HA NPs could be effectively ingested by cells in vitro.

Facilitating the endosomal escape and ensuring cytosolic delivery of the therapeutics is the key to achieve effective NPs-based therapy. Therefore, to investigate the lysosomes escape capabilities of HA NPs, a co-localization analysis of NPs with lysosomes in Colon-26 cells at different times was conducted. DiO (Green) was encapsulated in the NPs (HA-PS@NPs with CO_2 or HA-PS@NPs without CO_2), and lysosomes were stained with LysoTracker Red. The green fluorescence of DiO overlapped with the red fluorescence of LysoTracker Red

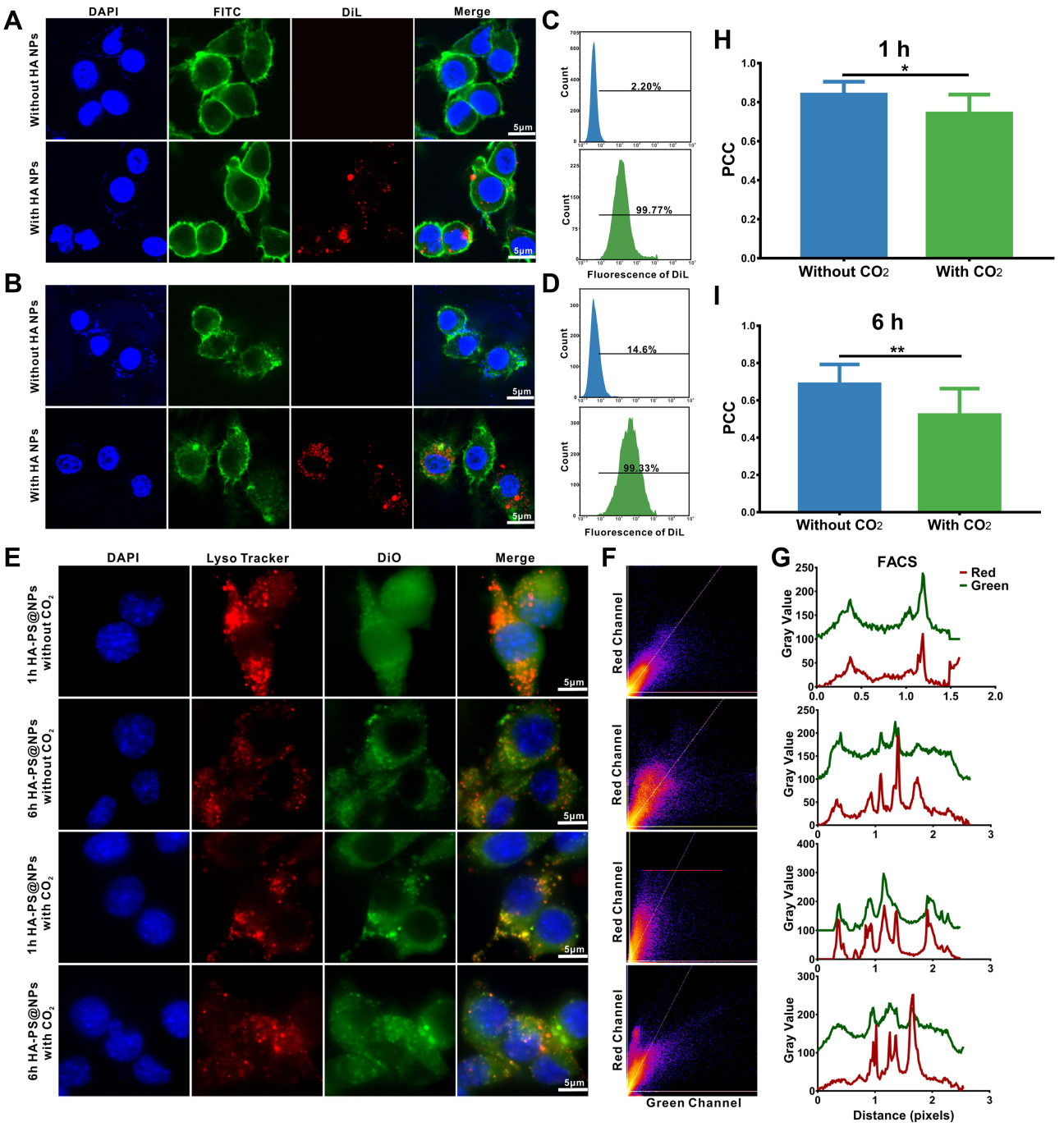

Figure 3 Cellular uptake of nanoparticles and low pH-activated lysosomal escape of HA-PS@NPs. (**A**) Colon-26 cells were incubated with DiL-labeled HA NPs, then stained by FITC-phalloidin and DAPI to visualize cytoskeleton and nucleus, respectively. (**B**) Raw 264.7 cells were incubated with DiL-labeled HA-NPs, then stained by FITC-phalloidin and DAPI to visualize cytoskeleton and nucleus, respectively. (**C**) Colon-26 cells uptake efficiency of NPs and HA NPs were measured using flow cytometry. (**D**) Raw 264.7 cells uptake efficiency of HA NPs were measured using flow cytometry. (**E**) Representative images of Colon-26 cells incubated with HA-PS@NPs with CO_2 and HA-PS@NPs without CO_2 for 1 h and 6 h at 37°C. The cell nuclei were stained by DAPI (blue), the lysosomes were stained by LysoTracker Red (red), and HA-PS@NPs were labeled with DiO (green). (**F**) Color scatter plots of HA-PS@NPs vs lysosomes. (**G**) Plot profiles of HA-PS@NPs vs lysosomes. (**H–I**) Corresponding Pearson's correlation coefficient (PCC) values of HA-PS@NPs vs lysosomes (mean ± standard deviation, n > 10) at 1h and 6h. *P < 0.05, **P < 0.01 with 95% confidence level from the unpaired t-test.

in the group of both 1 h and 6 h treated HA-PS@NPs without CO_2. In the group of treated HA-PS@NPs with CO_2, co-localization was significantly reduced, especially at 6 h, suggesting that HA-PS@NPs with CO_2 enabled successful escape from lysosome (Figure 3E).

Additionally, color scatter plots (Figure 3F), plot profiles (Figure 3G), and corresponding Pearson's correlation coefficient (PCC) values (Figure 3H and I) were used to provide a statistical correlation between the red and green fluorescence signals in the images. Firstly, for the color scatter plots, both in the "without CO_2" groups and the group of 1 h HA-PS@NPs with CO_2, the green fluorescence and red fluorescence were linearly distributed, indicating a certain degree of co-localization relationship. In contrast, it could be seen that the red and green fluorescent gray values were concave in the group of 6 h HA-PS@NPs with CO_2, indicating that the co-localization relationship between NPs and lysosomes was fragile (Figure 3F). Secondly, for the plot profile results, when compared the peak positions of red and green fluorescence in different groups, we found that the red and green peaks of the "without CO_2" groups were almost analogous, indicating a certain degree of co-localization. However, several peak positions in "with CO_2" groups were different, showing no co-localization at these positions (Figure 3G). Thirdly, the PCC value further verified this phenomenon. In both groups for 1 h and 6 h, the PCC values in groups of "with CO_2" were significantly lower than those groups of "without CO_2" (Figure 3H and I). Collectively, these results indicated that the pH-activated "nano-bomb effect" of HA-L-Arg-CO_2@NPs facilitated lysosomal escape for cytosolic delivery of PS.

Synergistic Effect of HA-PS@NPs to Reduce LPS-Induced Inflammation in vitro

It is widely believed that activated macrophages and leukocytes can produce abundant reactive oxygen species (ROS) during the development of colitis. Therefore, the level of ROS was positively correlated to the severity of inflammation. To evaluate the ROS scavenging ability of HA-PS@NPs, activated Raw 264.7 cells were treated with 2.7-dichlorodihydrofluorescein diacetate (DCFH-DA), which is a ROS probe and its green fluorescence intensity can reflect ROS level of cells (Supplementary Methods).[33] Results showed that positive control (Rosup) and LPS-induced group had strong green fluorescence. In contrast, the Negative group (normal cells) had negligible fluorescence, indicating that LPS induced Raw 264.7 cells to produce ROS (Figure 4A). When treated cells by HA-PS@NPs, the green fluorescence, which reflected ROS level, was significantly reduced (Figure 4A and B). To further verify the anti-inflammatory ability of HA-PS@NPs in vitro, we also investigated the mRNA levels of TNF-α, IL-6, and IL-1β in activated RAW 264.7 cells by quantitative RT-PCR (Primer sequences were shown in Table S1). Our results indicated that the expressions of TNF-α, IL-6, and IL-1β were significantly increased in the LPS-treated group. After being treated by HA-PS@NPs (equal to 20 μM of PS), the expression levels of these cytokines were significantly decreased. Surprisingly, HA NPs treatment alone could also substantially reduce the ROS level and mRNA levels of TNF-α, IL-6, and IL-1β (Figure 4C–E).

These data illustrated that this "nano-bomb" carrier successfully delivered PS into the cytoplasm and exerted its anti-inflammatory effect. HA-PS@NPs could attenuate LPS-induced inflammation of macrophages, including overexpressed pro-inflammatory cytokines and ROS. Interestingly, we found that HA NPs alone could attenuate LPS-induced inflammation of macrophages, which indicated a potential anti-inflammatory mechanism of L-Arg.

Biocompatibility Evaluation of HA NPs in vivo and in vitro

To determine the safety of this nano-bomb carrier, MTT assay, Calcein-AM/PI (propidium iodide) cell staining, and clone formation assay were carried out in vitro (Supplementary Methods). Negligible cytotoxicity was found in tested times and concentrations of nanocarriers (Figure S2a-d, Figures S3, and S4). Moreover, HA NPs did not affect the clone formation of HT-29 cells (Figure S5). The biocompatibility of HA NPs was further evaluated in healthy mice in vivo. The mice were orally administered chitosan/alginic acid hydrogel encapsulating HA NPs or the same amount of hydrogel as control every day for 7 consecutive days and observe for 30 days. At the end of the observation period, we collected the whole blood and serum for blood routine and biochemical analysis. The organs were stained by hematoxylin and eosin (H&E) for histology study. There was no significant decrease in the number of red blood cells, white blood cells, neutrophils, lymphocytes, platelets, hemoglobin (Figure 5A). Additionally, the damage indexes of liver (alanine aminotransferase (ALT) and aspartate aminotransferase (AST)), the indicators of renal function urea (UREA) and creatinine (CREA), and the damage indexes of heart creatine kinase (CK) and lactate dehydrogenase (LDH-1) were all detected. It could be seen that there was no evident difference in these indexes between the control and HA NPs groups (Figure 5A). These results indicated that HA NPs had excellent hemocompatibility. H&E stainings of vital organs revealed that HA NPs did not cause any clear signs of organ damage, the liver hepatocytes appeared normal, no myocardial fibrillary loss

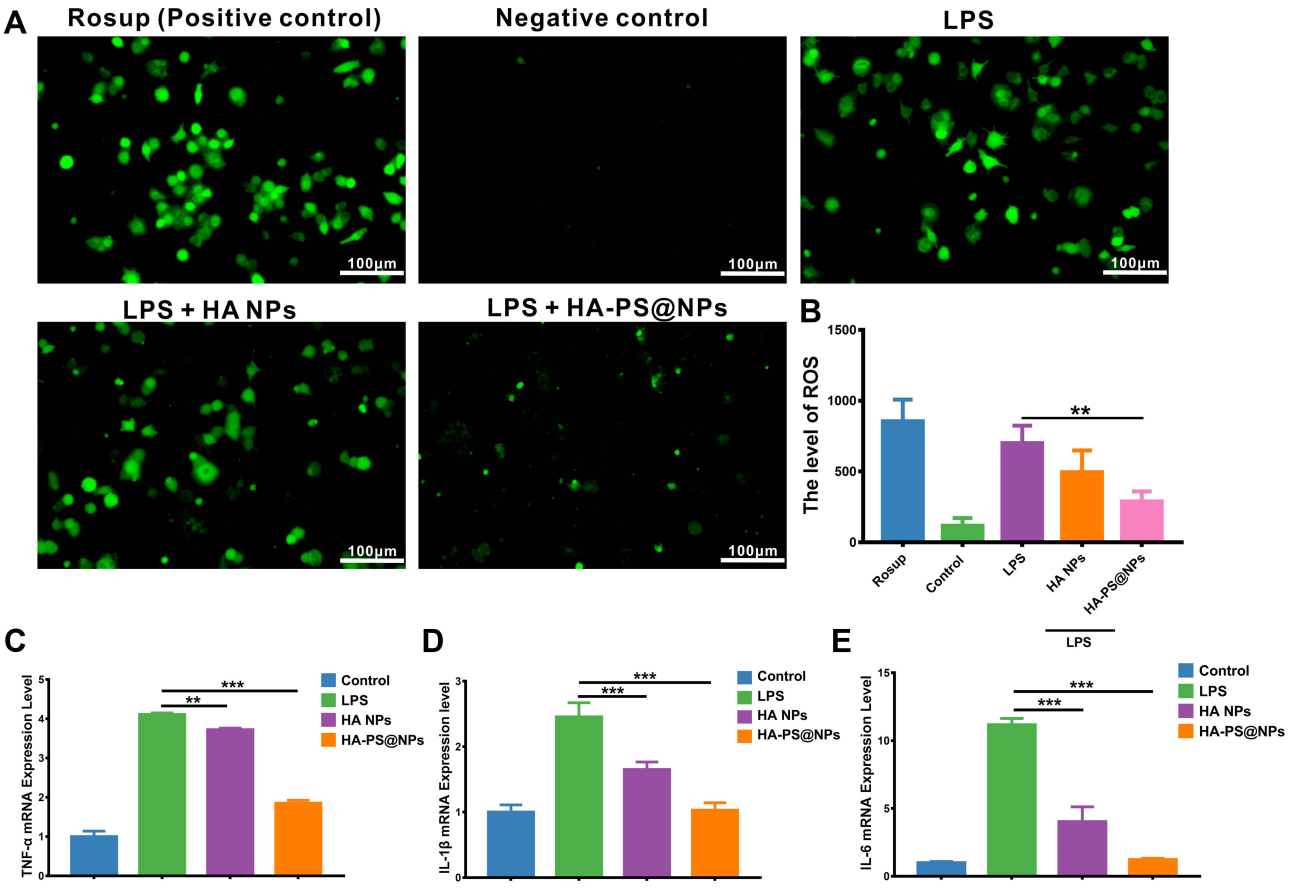

Figure 4 Synergistic effect of HA-PS@NPs to reduce LPS-induced macrophage inflammation. (**A**) ROS levels with different treatments were evaluated. ROS probe, DCFH-DA (10μM), was added to the cells and incubated for 30 min. Rosup (0.5mg/mL) treated group was a positive control. Fluorescence of cells was observed by fluorescence microscope with 488 nm excitation and 525nm emission. (**B**) The fluorescence intensity of each group was analyzed by Image J software, (n=6), $^{**}p<0.01$. (**C**–**E**) mRNAs expression of TNF-α, IL-1β and IL-6 in Raw 264.7 cells with different treatments were evaluated by real-time PCR, (n=6), $^{**}p<0.01$, $^{***}p<0.01$.

or vacuolation was observed in the heart, and no pulmonary fibrosis was detected in lung samples (Figure 5B). We also failed to find any notable toxicity sign in tissues from the GI tract (Figure S6). All the results proved evidence for the excellent biocompatibility of this "nano-bomb effect" carrier that was safely used as drug carriers.

Targeting Ability of HA NPs in vivo

HA could specifically target the CD44 receptor overexpressed on macrophages and colonic epithelial cells during colitis. To more intuitively observe the targeting ability of HA NPs to the inflamed colon in vivo compared with NPs. Normal and colitic mice were gavaged with NPs/DiR and HA NPs/DiR, respectively. At 12 h post-administration, the GI tract in each group was collected and imaged by VISQUE Invivo Smart-LF animal live imaging system. The HA NPs treated group exhibited stronger DiR signal in the colon compared with NPs both in normal and colitic mice (Figure 6). In other organs, DiR signal was almost negligible (Figure S7). These results suggested that HA modification enhanced the NPs uptake by colonic cells, increasing the targeting ability of NPs to the inflamed colon tissue. And HA NPs had good biological safety because they were not distributed to other organs except for the colon after oral administration.

Oral Administration of HA-PS@NPs in Hydrogel Attenuated DSS-Induced UC

The therapeutic effect of HA-PS@NPs against DSS-induced acute colitis in mice was evaluated. The mice were divided into 4 groups and received regular water (control), 2% (w/v) of DSS (DSS group), hydrogel encapsulated with HA NPs (500mg/kg), hydrogel encapsulated with HA-PS@NPs (500mg/kg, equal to 40mg/kg PS) (Figure 7A). Compared with the DSS group, HA-PS@NPs treatment significantly increase mice's body weight and colon length and decrease the

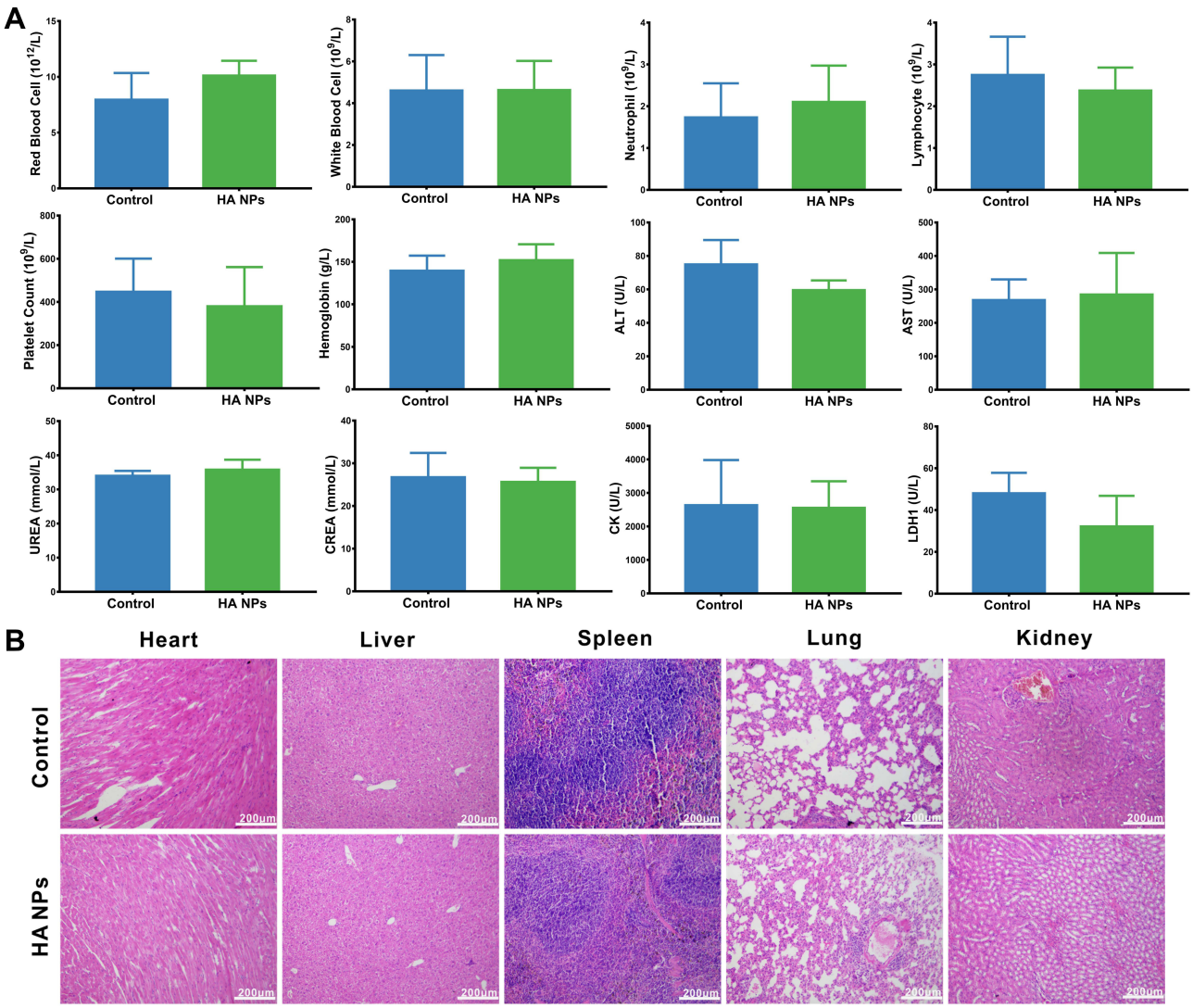

Figure 5 Biocompatibility evaluation of HA NPs in vitro and in vivo. (**A**) The counts' changes of Red blood cell, White blood cell, Neutrophil, Lymphocyte Platelet, Hemoglobin, alanine aminotransferase (ALT), aspartate aminotransferase (AST), urea (UREA) and creatinine (CREA), creatine kinase (CK) and lactate dehydrogenase (LDH-1) (n=6). (**B**) H&E staining of vital organs (heart, liver, spleen, lung, kidney) was used to assess the systemic toxicity of HA NPs.

disease activity index (DAI) in the DSS-colitis mice (Figures 7B-D and S8). The intestinal barrier functions were analyzed using FITC-labeled dextran, the serum concentrations of dextran-FITC were decreased in the HA-PS@NPs group compared with the DSS group (Figure 7E). It was worth noting that HA NPs treatment also showed a certain trend of relieving colitis, but there was no statistical difference. In terms of molecular biology and histology, the mRNA expression levels of the pro-inflammatory cytokine, including TNF-α, and IL-1β, IL-6, and IL-12 were significantly decreased after HA NPs and HA-PS@NPs treatment (Figure 7F–I). And histological changes of HA-PS@NPs against DSS-induced UC were observed by the H&E staining method. Mice treated with DSS alone exhibited robust signs of inflammation, including epithelial erosion, interstitial edema, and a general increase in the number of inflammatory cells in the lamina propria. In contrast, mice treated with HA-PS@NPs significantly attenuated DSS-induced colonic inflammation, epithelial damage, and crypt shortening in mice (Figure 7J and K).

To further evaluate the antioxidant effect of HA-PS@NPs in mice, we used the Reactive Oxygen Species (ROS) Assay kit of DCFH-DA (Beyotime) to incubate with colonic tissues and frozen sections of colon from mice in different treatment groups. Results showed that DSS treatment group had strong fluorescence intensity, which indicated the overexpression of ROS. In contrast, the control group had negligible fluorescence, indicating that DSS induced the

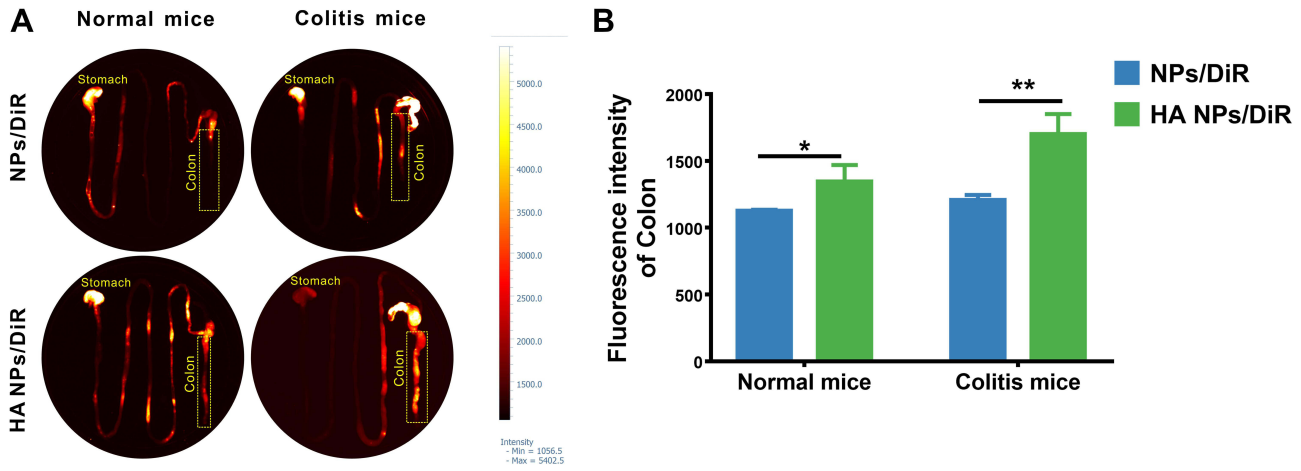

Figure 6 In vivo inflammation targeting of HA NPs in colitis mice. In vivo inflammation targeting of HA NPs in colitis mice. (**A**) DiR-labeled NPs and HA NPs were orally administrated to colitic mice and healthy controls. Images were obtained at 12 h post-administration using the VISQUE Invivo Smart-LF animal live imaging system. (**B**) Fluorescence intensities of the region of interest (ROI) were quantified with an imaging system (n=3), *p<0.05, **p<0.01.

production of large amounts of ROS. When treated mice by HA-PS@NPs, the fluorescence intensity, which reflected ROS level, was significantly reduced (Figures S9 and S10). These results further manifested that the CA hydrogel delivered NPs to the colon, and oral administration of HA-PS@NPs attenuated DSS-induced colitis in vivo.

Discussion

Various colon-targeted nano-drug delivery systems have been designed for the treatment of UC by recent developments in nanotechnology. Advantageous features include the potential to augment local drug concentrations in inflamed tissue, improving drug efficacy, decreasing dosing frequency, reduce drug unwanted side effects, and the ability to enhance the solubility of hydrophobic molecules.[34–36] However, successful cytosolic delivery of nanomaterials is still a challenge in designing effective nanoparticle delivery systems.[37] Nanoparticles are typically internalized into cells through the endocytosis pathway, which involves internalization into an endocytic vesicle, fusion into the early endosome, maturation into the late endosome, and accumulation in the lysosome. During the progress of endosome maturation, the pH decreases from physiological pH of 7.4 down to ~pH 6.5 in the early endosome, ~pH 6.0 in the late endosome, and ~pH 5.0 in the lysosome.[38]

The nanoparticles remain trapped in these compartments, and the environment of the lysosome can result in significant degradation of the therapeutic cargo. Thus, releasing from these compartments is essential for improved efficacy of drugs.[39] Currently, several strategies have been designed to facilitate endosomal escape, such as pH-sensitive anionic endosmotic agents, cationic endosmotic agents, and modification of lipid or polymer nanoparticles.[40,41] However, these strategies often suffered from potential toxicity, high cost, and convoluted synthesis/conjugation processes.

In our present study, we designed a pH-activated nano-bomb drug delivery system by using the natural guanidine group in L-Arginine, in which the guanidine group adsorbed CO_2 in neutral pH conditions and release CO_2 in acidic pH conditions. The released CO_2 broke the lysosome and successfully delivered the loaded drugs to the cytoplasm. And it had the advantages of synthetic steps, good biocompatibility, and high selectivity. The loading of L-Arginine did not affect the PS encapsulation efficiency (79±4.58%) and loading efficiency (11.67±1.42%).

The production of pro-inflammatory cytokines and reactive oxygen species (ROS) produced by activated macrophages and leukocytes during the development of colitis was directly correlated to the inflammation.[33,42] LPS was used to activate Raw 264.7 cells to mimic acute inflammation model in vitro as the combination of LPS and toll-like receptors (TLRs) on the surface of immune cells activates the intracellular protein kinases (MAPKs) and nuclear factor-kB (NF-κB) signaling pathways, producing associated pro-inflammatory cytokines and ROS.[43] In our study, HA-PS@NPs

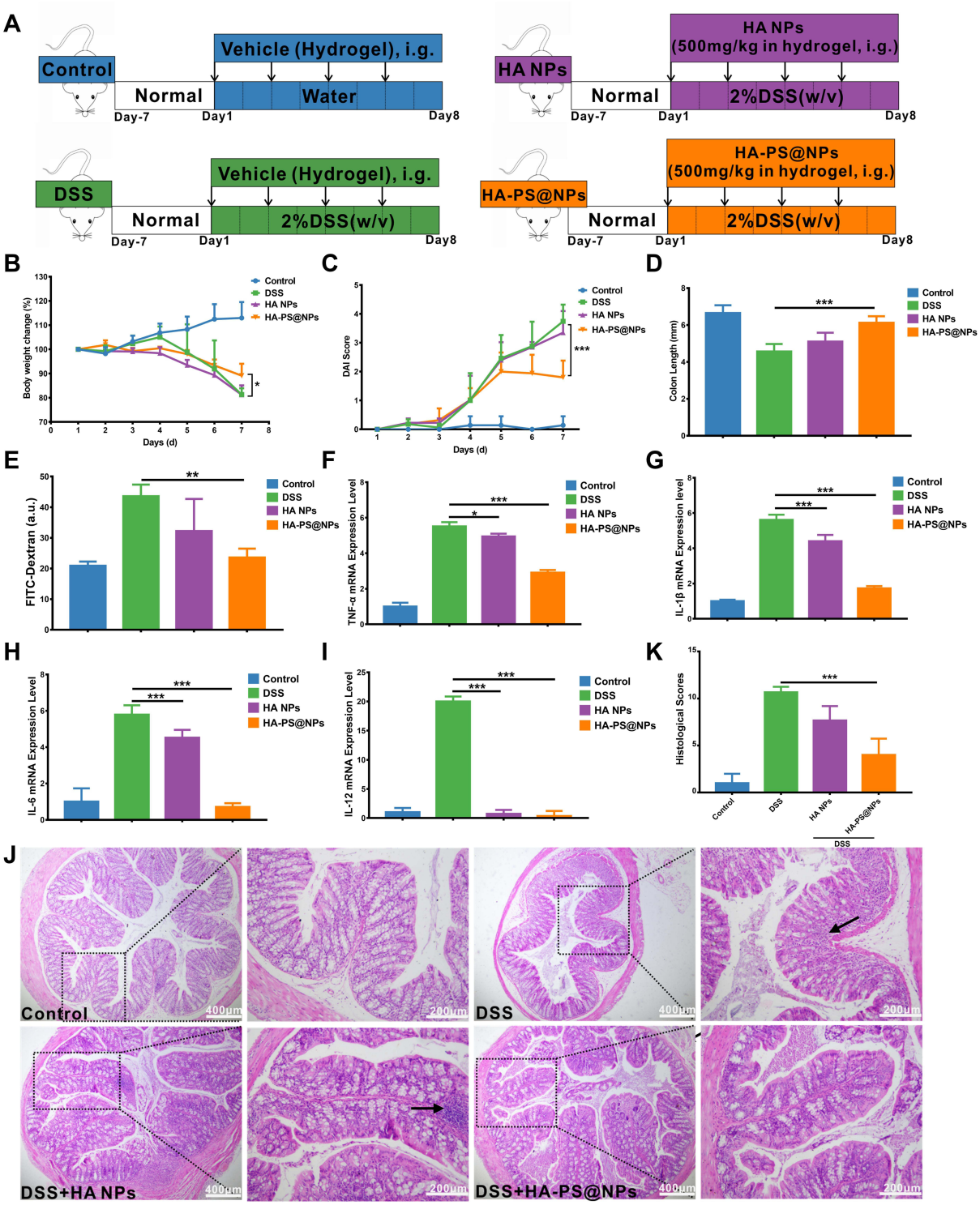

Figure 7 Oral administration of HA NPs and HA-PS@NPs yields an enhanced therapeutic efficacy against DSS-induced UC. (**A**) Schematic illustration of the murine model of colitis induced by 2% DSS along with NPs treatment at 500 mg/kg (PS 40mg/kg) for consecutive 7 days. Mice were orally administrated with hydrogel or hydrogel encapsulated of HA NPs and HA-PS@NPs every other day. The daily changes in body weight (n=6) (**B**) and disease activity index (DAI) (**C**) of the mice during a 7-day treatment course. (**D**) Colon length change of different treatment groups (n=6). (**E**) HA-PS@NPs significantly reduces epithelial permeability in UC. The mice were gavaged with FITC-dextran (40 mg/100 g body weight) and blood was collected 5 hours later. The serum concentration of FITC-dextran was quantified by a fluorescence Spectrometer (485/528 nm) (n=5), *p<0.05, **p<0.01, ***p<0.01. (**F–I**) The mRNA expression levels of TNF-α, IL-1β, IL-6, IL-12 (n=6). *p<0.05, ***p<0.01. (**J**) Hematoxylin and eosin staining for microscopic evaluation of the colon sections isolated from healthy control, DSS, HA NPs and HA-PS@NPs treated groups. Images of tissues are shown with 4× and 100× magnification, (n=10/group). Arrowheads indicate inflammatory cells in the lamina propria. (**K**) Histological scores from the different treatment groups were calculated (n=6). ***p<0.001.

significantly reduced the mRNA expression of pro-inflammatory cytokine and the production of ROS, indicating that it had an excellent anti-inflammatory effect in vitro.

Furthermore, oral administration HA-PS@NPs in the mouse UC model in our study could also significantly relieve colitis symptoms by reducing intestinal barrier permeability and downregulating the expression of pro-inflammatory cytokine, which should be attributed to the effect of PS. As previously reported, PS pretreatment markedly ameliorated intestinal barrier dysfunction caused by DSS by preventing myosin light-chain kinase (MLCK) from driving phosphorylation of MLC (p-MLC) in DSS-induced colitis mice.[44] Furthermore, PS could also ameliorate colonic inflammation via suppressing dendritic cell activation, promoting regulatory T cell development, and regulating the gut microbiota.[45]

Compared with intravenous administration (i.v.), oral administration has incomparable advantages in enhancing patient compliance, avoiding side effects from the long-term intravenous injection, and improving patients' quality of life.[46,47] The chitosan/alginate (CA) hydrogel we selected could successfully deliver HA-PS@NPs to the colon overcoming the complex microenvironment of the gastrointestinal tract. Furthermore, HA modification increased the ability of NPs to target the inflamed colon tissue. CD44, a single-chain transmembrane glycoprotein with a molecular mass of 80 to 250kD, is overexpressed on the surface of colon epithelial cells and macrophages in UC tissues. HA can selectively bind to CD44 and block its release of a drug because of its large and biocompatible molecular size, not to mention its ability to be readily degraded by HAase after being taken up by cells.[48]

Interestingly, HA NPs loaded with L-Arg could also reduce the expression of pro-inflammatory cytokines both in vitro and in vivo to a certain extent, which was consistent with previous report.[49,50] Shreds of evidence show that L-Arginine regulates the progression of IBD through the oxidative system, intestinal immunity, intestinal microbiota, tight junction proteins, and metabolic products, like nitric oxide (NO) and polyamines.[21,51] L-Arg is metabolized by nitric oxide synthase (NOS), which generates NO and L-citrulline. NO regulates the immune response during inflammation as an essential immune-modulator and maintains the integrity of intestinal mucosal barrier structure and function.[52] And L-Arg also serves as a precursor to glutamine, proline, and ornithine, with the latter serving as the substrate for synthesizing polyamines. Polyamines are associated with mucosal protection in the gastrointestinal tract.[49] Both of them regulate inflammation through the phosphoinositide-3-kinases (PI3K)/PI3K-protein kinase B (Akt) and the myosin light-chain kinase (MLCK)-myosin light chain (MLC20) pathway in the colon.[44] The specific mechanism needs further verification in our study.

Conclusion

In this study, we developed an HA-modified pH-activated nano-bomb system loaded with PS (HA-PS@NPs) for UC treatment. Under lysosomal acidic pH conditions, L-Arginine-CO_2 (L-Arg-CO_2) in HA-L-Arg-CO_2@NPs carrier released CO_2 and produced a "nano-bomb effect" to trigger PS lysosomal escape. HA-L-Arg-CO_2@NPs targeted the inflammation colon efficiently via CD44 receptors, which overexpressed in macrophages and colonic epithelial cells. By down-regulating the expression of pro-inflammatory cytokines, HA NPs and HA-PS@NPs reduced inflammation and alleviated UC symptoms by oral administration. In conclusion, this pH-activated nano-bomb drug delivery system with a therapeutic effect provides a practical targeting strategy for UC treatment.

Data Sharing Statement

The data underlying this article are available in the article and in its online Supplementary Material.

Acknowledgments

This work was supported by the National Natural Science Foundation of China (No. 82000523, 32171392), Shaanxi Province's Science and Technology Innovation Team Program for Immune-related diseases (2021TD-38), the Natural Science Foundation of Shaanxi Province of China (Nos. 2020JQ-087, 2020JQ-095, 2021JQ-009), the "Young Talent Support Plan" of Xi'an Jiaotong University, China (No. YX6J001). We also thank Dr. Zijun Ren at the Instrument Analysis Center of Xi'an Jiaotong University for assisting with TEM analysis.

Author Contributions

All authors made a significant contribution to the work reported, whether that is in the conception, study design, execution, acquisition of data, analysis and interpretation, or in all these areas; took part in drafting, revising or critically reviewing the article; gave final approval of the version to be published; have agreed on the journal to which the article has been submitted; and agree to be accountable for all aspects of the work.

Disclosure

The authors report no conflicts of interest in this work.

References

1. Ungaro R, Colombel JF, Lissoos T, Peyrin-Biroulet L. A treat-to-target update in ulcerative colitis: a systematic review. *Am J Gastroenterol*. 2019;114(6):874–883. doi:10.14309/ajg.0000000000000183
2. Rubin DT, Ananthakrishnan AN, Siegel CA, Sauer BG, Long MD. ACG clinical guideline: ulcerative colitis in adults. *Am J Gastroenterol*. 2019;114(3):384–413.
3. Hartwig O, Shetab Boushehri MA, Shalaby KS, Loretz B, Lamprecht A, Lehr CM. Drug delivery to the inflamed intestinal mucosa - targeting technologies and human cell culture models for better therapies of IBD. *Adv Drug Deliv Rev*. 2021;175:113828.
4. Zheng K, Jia J, Yan S, Shen H, Zhu P, Yu J. Paeoniflorin ameliorates ulcerative colitis by modulating the dendritic cell-mediated TH17/Treg balance. *Inflammopharmacology*. 2020;28(6):1705–1716.
5. Gajendran M, Loganathan P, Jimenez G, et al. A comprehensive review and update on ulcerative colitis. *Dis Mon*. 2019;65(12):100851.
6. Tripathi K, Feuerstein JD. New developments in ulcerative colitis: latest evidence on management, treatment, and maintenance. *Drugs Context*. 2019;8:212572. doi:10.7573/dic.212572
7. Pagnini C, Pizarro TT, Cominelli F. Novel pharmacological therapy in inflammatory bowel diseases: beyond anti-tumor necrosis factor. *Front Pharmacol*. 2019;10:671.
8. Shi H, Zhao X, Gao J, et al. Acid-resistant ROS-responsive hyperbranched polythioether micelles for ulcerative colitis therapy. *Chinese Chem Letters*. 2020;31(12):3102–3106. doi:10.1016/j.cclet.2020.03.039
9. Mitchell MJ, Billingsley MM, Haley RM, Wechsler ME, Peppas NA, Langer R. Engineering precision nanoparticles for drug delivery. *Nat Rev Drug Discov*. 2021;20(2):101–124.
10. Chen F, Liu Q, Xiong Y, Xu L. Current strategies and potential prospects of nanomedicine-mediated therapy in inflammatory bowel disease. *Int J Nanomedicine*. 2021;16:4225–4237. doi:10.2147/IJN.S310952
11. Yu W, Shevtsov M, Chen X, Gao H. Advances in aggregatable nanoparticles for tumor-targeted drug delivery. *Chinese Chem Letters*. 2020;31(6):1366–1374. doi:10.1016/j.cclet.2020.02.036
12. Lonn P, Kacsinta AD, Cui XS, et al. Enhancing endosomal escape for intracellular delivery of macromolecular biologic therapeutics. *Sci Rep*. 2016;6:32301. doi:10.1038/srep32301
13. Liu Y, Xu J, Choi HH, et al. Targeting 17q23 amplicon to overcome the resistance to anti-HER2 therapy in HER2+ breast cancer. *Nat Commun*. 2018;9(1):4718.
14. Xu J, Liu Y, Li Y, et al. Precise targeting of POLR2A as a therapeutic strategy for human triple negative breast cancer. *Nat Nanotechnol*. 2019;14(4):388–397. doi:10.1038/s41565-019-0381-6
15. Chen J, Li J, Zhou J, et al. Metal-phenolic coatings as a platform to trigger endosomal escape of nanoparticles. *ACS Nano*. 2019;13(10):11653–11664. doi:10.1021/acsnano.9b05521
16. Qin Y, Guo Q, Wu S, et al. LHRH/TAT dual peptides-conjugated polymeric vesicles for PTT enhanced chemotherapy to overcome hepatocellular carcinoma. *Chinese Chem Letters*. 2020;31(12):3121–3126. doi:10.1016/j.cclet.2020.06.023
17. Hong SK, Maltz BE, Coburn LA, et al. Increased serum levels of L-arginine in ulcerative colitis and correlation with disease severity. *Inflamm Bowel Dis*. 2010;16(1):105–111. doi:10.1002/ibd.21035
18. Coburn LA, Gong X, Singh K, et al. L-arginine supplementation improves responses to injury and inflammation in dextran sulfate sodium colitis. *PLoS One*. 2012;7(3):e33546. doi:10.1371/journal.pone.0033546
19. Andrade MER, Santos RDGCD, Soares ADN, et al. Pretreatment and treatment with L-arginine attenuate weight loss and bacterial translocation in dextran sulfate sodium colitis. *JPEN J Parenter Enteral Nutr*. 2016;40(8):1131–1139. doi:10.1177/0148607115581374
20. Singh K, Gobert AP, Coburn LA, et al. Dietary arginine regulates severity of experimental colitis and affects the colonic microbiome. *Front Cell Infect Microbiol*. 2019;9:66. doi:10.3389/fcimb.2019.00066
21. Baier J, Gansbauer M, Giessler C, et al. Arginase impedes the resolution of colitis by altering the microbiome and metabolome. *J Clin Invest*. 2020;130(11):5703–5720. doi:10.1172/JCI126923
22. Chen Y, Park J, Joe Y, et al. Pterostilbene 4'-beta-glucoside protects against dss-induced colitis via induction of tristetraprolin. *Oxid Med Cell Longev*. 2017;2017:9427583. doi:10.1155/2017/9427583
23. Shi L, Liu Q, Tang J-H, Wen -J-J, Li C. Protective effects of pterostilbene on ulcerative colitis in rats via suppressing NF-κB pathway and activating PPAR-γ. *Eur J Inflamm*. 2019;17:2058739219840152.
24. Laroui H, Sitaraman SV, Merlin D. A method to target bioactive compounds to specific regions of the gastrointestinal tract: double gavage using polysaccharide hydrogels. *Protocol Exchange*. 2009.
25. Laroui H, Dalmasso G, Nguyen HT, Yan Y, Sitaraman SV, Merlin D. Drug-loaded nanoparticles targeted to the colon with polysaccharide hydrogel reduce colitis in a mouse model. *Gastroenterology*. 2010;138(3):843–53e1-2. doi:10.1053/j.gastro.2009.11.003
26. Xiao B, Zhang Z, Viennois E, et al. Combination therapy for ulcerative colitis: orally targeted nanoparticles prevent mucosal damage and relieve inflammation. *Theranostics*. 2016;6(12):2250–2266. doi:10.7150/thno.15710

27. Xiao B, Viennois E, Chen Q, et al. Silencing of intestinal glycoprotein CD98 by orally targeted nanoparticles enhances chemosensitization of colon cancer. *ACS Nano*. 2018;12(6):5253–5265. doi:10.1021/acsnano.7b08499
28. Dou YX, Zhou JT, Wang TT, et al. Self-nanoemulsifying drug delivery system of bruceine D: a new approach for anti-ulcerative colitis. *Int J Nanomedicine*. 2018;13:5887–5907. doi:10.2147/IJN.S174146
29. Yang M, Zhang F, Yang C, et al. Oral targeted delivery by nanoparticles enhances efficacy of an HSP90 inhibitor by reducing systemic exposure in murine models of colitis and colitis-associated cancer. *J Crohns Colitis*. 2020;14(1):130–141. doi:10.1093/ecco-jcc/jjz113
30. Tian H, He Z, Sun C, et al. Uniform core-shell nanoparticles with thiolated hyaluronic acid coating to enhance oral delivery of insulin. *Adv Healthc Mater*. 2018;7(17):e1800285. doi:10.1002/adhm.201800285
31. Deng J, Wu Z, Zhao Z, et al. Berberine-loaded nanostructured lipid carriers enhance the treatment of ulcerative colitis. *Int J Nanomedicine*. 2020;15:3937–3951. doi:10.2147/IJN.S247406
32. Xiao YT, Yan WH, Cao Y, Yan JK, Cai W. Neutralization of IL-6 and TNF-alpha ameliorates intestinal permeability in DSS-induced colitis. *Cytokine*. 2016;83:189–192. doi:10.1016/j.cyto.2016.04.012
33. Chen L, You Q, Hu L, et al. The antioxidant procyanidin reduces reactive oxygen species signaling in macrophages and ameliorates experimental colitis in mice. *Front Immunol*. 2017;8:1910. doi:10.3389/fimmu.2017.01910
34. Naeem M, Bae J, Oshi MA, et al. Colon-targeted delivery of cyclosporine A using dual-functional Eudragit((R)) FS30D/PLGA nanoparticles ameliorates murine experimental colitis. *Int J Nanomedicine*. 2018;13:1225–1240. doi:10.2147/IJN.S157566
35. Sun Y, Duan B, Chen H, Xu X, Novel A. Strategy for treating inflammatory bowel disease by targeting delivery of methotrexate through glucan particles. *Adv Healthc Mater*. 2020;9(6):e1901805.
36. Ji W, Zhang T, Lu Z, Shen J, Xiao Z, Zhang X. Synthesis and characterization of novel biocompatible nanocapsules encapsulated lily fragrance. *Chinese Chem Letters*. 2019;30(3):739–742. doi:10.1016/j.cclet.2018.09.008
37. Martens TF, Remaut K, Demeester J, De Smedt SC, Braeckmans K. Intracellular delivery of nanomaterials: how to catch endosomal escape in the act. *Nano Today*. 2014;9(3):344–364. doi:10.1016/j.nantod.2014.04.011
38. Smith SA, Selby LI, Johnston APR, Such GK. The endosomal escape of nanoparticles: toward more efficient cellular delivery. *Bioconjug Chem*. 2019;30(2):263–272. doi:10.1021/acs.bioconjchem.8b00732
39. Cupic KI, Rennick JJ, Johnston AP, Such GK. Controlling endosomal escape using nanoparticle composition: current progress and future perspectives. *Nanomedicine*. 2019;14:215–223. doi:10.2217/nnm-2018-0326
40. Ahmad A, Khan JM, Haque S. Strategies in the design of endosomolytic agents for facilitating endosomal escape in nanoparticles. *Biochimie*. 2019;160:61–75.
41. Zheng P, Liu Y, Chen J, Xu W, Li G, Ding J. Targeted pH-responsive polyion complex micelle for controlled intracellular drug delivery. *Chinese Chem Letters*. 2020;31(5):1178–1182. doi:10.1016/j.cclet.2019.12.001
42. Vong LB, Yoshitomi T, Morikawa K, Saito S, Matsui H, Nagasaki Y. Oral nanotherapeutics: effect of redox nanoparticle on microflora in mice with dextran sodium sulfate-induced colitis. *J Gastroenterol*. 2014;49(5):806–813. doi:10.1007/s00535-013-0836-8
43. Wang W, Liu P, Hao C, Wu L, Wan W, Mao X. Neoagaro-oligosaccharide monomers inhibit inflammation in LPS-stimulated macrophages through suppression of MAPK and NF-kappaB pathways. *Sci Rep*. 2017;7:44252. doi:10.1038/srep44252
44. Wang J, Zhao H, Lv K, et al. Pterostilbene Ameliorates dss-induced intestinal epithelial barrier loss in mice via suppression of the NF-kappaB-mediated MLCK-MLC signaling pathway. *J Agric Food Chem*. 2021;69(13):3871–3878.
45. Yashiro T, Yura S, Tobita A, Toyoda Y, Kasakura K, Nishiyama C. Pterostilbene reduces colonic inflammation by suppressing dendritic cell activation and promoting regulatory T cell development. *FASEB J*. 2020;34(11):14810–14819. doi:10.1096/fj.202001502R
46. Zhang M, Merlin D. Nanoparticle-based oral drug delivery systems targeting the colon for treatment of ulcerative colitis. *Inflamm Bowel Dis*. 2018;24(7):1401–1415.
47. Duan B, Li M, Sun Y, Zou S, Xu X. Orally delivered antisense oligodeoxyribonucleotides of TNF-alpha via polysaccharide-based nanocomposites targeting intestinal inflammation. *Adv Healthc Mater*. 2019;8(5):e1801389. doi:10.1002/adhm.201801389
48. Yang M, Zhang Y, Ma Y, et al. Nanoparticle-based therapeutics of inflammatory bowel diseases: a narrative review of the current state and prospects. *J Bio-X Res*. 2020;3(4):157–173.
49. Meng Q, Cooney M, Yepuri N, Cooney RN. L-arginine attenuates Interleukin-1beta (IL-1beta) induced Nuclear Factor Kappa-Beta (NF-kappaB) activation in Caco-2 cells. *PLoS One*. 2017;12(3):e0174441. doi:10.1371/journal.pone.0174441
50. Qiu Y, Yang X, Wang L, Gao K, Jiang Z. L-arginine inhibited inflammatory response and oxidative stress induced by lipopolysaccharide via arginase-1 signaling in IPEC-J2 cells. *Int J Mol Sci*. 2019;20:7. doi:10.3390/ijms20071800
51. Andrade MER, Barros P, Menta P, et al. Arginine supplementation reduces colonic injury, inflammation and oxidative stress of DSS-induced colitis in mice. *J Funct Foods*. 2019;52:360–369. doi:10.1016/j.jff.2018.11.019
52. Krzystek-Korpacka M, Fleszar MG, Bednarz-Misa I, et al. Transcriptional and metabolomic analysis of L-arginine/nitric oxide pathway in inflammatory bowel disease and its association with local inflammatory and angiogenic response: preliminary findings. *Int J Mol Sci*. 2020;21:5. doi:10.3390/ijms21051641